PERSISTENT CURRENT EFFECTS IN RHIC Arc DIPOLE MAGNETS OPERATED AT LOW CURRENTS*

X. Wang†, S. Caspi, S. A. Gourlay, G.L. Sabbi, LBNL, Berkeley, CA 94720, USA
A. K. Ghosh, R. C. Gupta, A. K. Jain, P. Wanderer, BNL, Upton, NY 11973, USA

Abstract

The Relativistic Heavy Ion Collider (RHIC) arc dipoles at Brookhaven National Laboratory are operated at low field for low energy Au-Au studies. Indications of strong nonlinear magnetic fields have been observed at these low currents due to the persistent current effects of superconducting NbTi filaments. We report the details of the measurement and calculation of the field errors due to persistent current effect. The persistent current induced field errors calculated with a model based on the strand magnetization data agree well with the measurements of a spare arc dipole magnet. The dependence of the persistent current effects on the park current is calculated based on the validated model.

INTRODUCTION

The arc dipole magnets of the Relativistic Heavy Ion Collider (RHIC) at Brookhaven National Laboratory (BNL) are operated at low currents (112 to 218 A) for low energy Au-Au studies. Strong non-linear magnetic fields have been observed at these low currents. These non-linear fields result from the magnetization of superconducting filaments in the magnet conductor (persistent current effect). To understand the magnetization effects and achieve the best machine performance, the field errors were measured using a spare arc dipole magnet at low currents and compared to a computational model. Here we describe the model and the comparison with measurements. With the validated model, we calculate the dependence of the persistent current effect on the park current from which the current starts ramping up toward the operation current after the down ramp. Adjusting the park current can be an option to optimize the RHIC performance at low operation energy.

The RHIC arc dipole was wound with Rutherford cables made of multifilamentary NbTi strands. Table 1 summarizes the NbTi strand parameters relevant for the persistent current effects. Reference [1] reviews the RHIC magnet system, including the conductor, cable and arc dipole.

MAGNETIC MODEL

Several models have been developed to calculate the persistent current effects for superconducting accelerator magnets based on NbTi and Nb_3Sn conductors [2–8]. Here we use an analytic approach based on the critical state model [9, 10] to calculate the persistent current effects [2].

Table 1: Main Parameters for the NbTi Strands Used in the RHIC Arc Dipole Magnets

Item		Value
Wire diameter (mm)	d_W	0.648
Filament diameter (μm)	d_F	6
Filament number in a strand	N_F	3510
Cu/Non-Cu ratio	λ	2.25
Strand number in a cable	N_S	30

The magnetic field in the straight section of a long dipole magnet is two dimensional (2D). On the 2D magnet cross section, each strand is approximated as a line current located at the strand center. The field on each strand is first determined by summing the field generated by all other strands using the Biot-Savart law. This field then determines the induced persistent current in each filament of the strand. The sum of the fields generated by the persistent current in each filament gives the strand contribution to the persistent current effect.

Two parameters are required to determine the persistent current effect from each filament. The first one is the shape of the shielding currents in the superconducting filament before it is fully penetrated by the external magnetic field. We approximate the central region in the filament, initially current free, to an ellipse using Wilson's model [2, 11]. The eccentricity of the ellipse, ϵ, can be determined by

$$B_s = -\frac{\mu_0 J_c d_F}{\pi}\left(1 - \sqrt{1-\epsilon^2}\,\frac{\arcsin\epsilon}{\epsilon}\right), \qquad (1)$$

where B_s is the field generated by the shielding current at the center of the filament to cancel the applied field [2]. J_c is the critical current density of the NbTi filament and d_F is the filament diameter (Table 1). The eccentricity can be determined based on a series expansion of the tangent function [12, 13].

The second parameter is the filament J_c as a function of applied field, which can be determined from the strand magnetization [14]. For a filament fully penetrated by external magnetic field, its magnetization and J_c can be related through

$$M(B) = \frac{2}{3\pi} J_c(B)\, d_F\, \frac{1}{1+\lambda}, \qquad (2)$$

where λ is the Cu/Non-Cu ratio (Table 1) [2]. Two sets of $J_c(B)$ data can be obtained from the measured strand magnetization: one from the up-ramp branch with increasing applied magnetic field and the other from the down-ramp branch. We then approximate the $J_c(B)$ data with the

7: Accelerator Technology Main Systems

T10 - Superconducting Magnets

Schwerg-Völlinger formula to facilitate the magnetization calculation [15].

A fortran code was developed to calculate the geometric and persistent current field errors. The field generated by the image of each line current is considered at low field when the iron yoke is not saturated. The code neglects the effect of transport current on the strand magnetization [2].

MEASUREMENT OF PERSISTENT CURRENT INDUCED FIELD ERRORS

Measurement Setup and Protocol

The field errors were measured at BNL with a spare D96 arc dipole magnet in liquid helium bath at 4.3 K. The magnet is 2.97 m long and the measurements were performed covering the central 1 m of the body. Harmonics were measured with a rotating coil with 1.32 s time resolution [16].

The magnetization history is first standardized by carrying out three AC cycles between 50 A (park current) and 1948 A as per ramp profile specified. Each cycle consists of a) ramp up from 50 A to the operating current (I_{op}), b) a wait at I_{op}, c) ramp up from I_{op} to 1948 A, d) a wait at 1948 A, e) ramp down from 1948 A to I_{op}, f) a wait at I_{op}, g) ramp down from I_{op} to 50 A, and h) a wait at 50 A. The ramp details depend on the chosen operating current as specified in the run plan. The magnet current was then ramped from 50 A to one of the operating currents, as per the specified ramp profile. A full "DC Loop" was measured at various current steps from 50 to 1948 A.

The magnetic field in the aperture of the magnet straight section can be expressed as

$$B_y + i\,B_x = \sum_{n=1}^{\infty} (B_n + iA_n) \left(\frac{z}{R_{ref}}\right)^{n-1}, \qquad (3)$$

where z is a vector on the 2D complex plane. $B_n + iA_n$ is the multipole of order n in Tesla at the reference radius R_{ref} [17]. Here we use a reference radius of 25 mm (magnet aperture 80 mm). Multipoles normalized to the main dipole field component B_1 (with $A_1 = 0$) are given by $b_n + ia_n = 10^4 (B_n + iA_n)/B_1$.

Measurement Results

Figure 1 shows the dipole transfer function from the "DC loop" measurements. The dashed line at 0.708 T/kA in Fig. 1 is the geometric transfer function with no persistent current effect or iron saturation. The persistent current effect in the transfer function is evidenced with two observations: the increased transfer function below 200 A and the hysteresis between the up and down ramps. The iron yoke started saturating at around 1100 A.

We expect the persistent current effect to affect only the allowed harmonics if every strand on the magnet cross section has the same magnetization as a function of applied field. In reality, differences of the strand magnetization, even though small, lead to non-allowed field errors. For instance, there is about 1 unit of quadrupole below 100 A for the measured
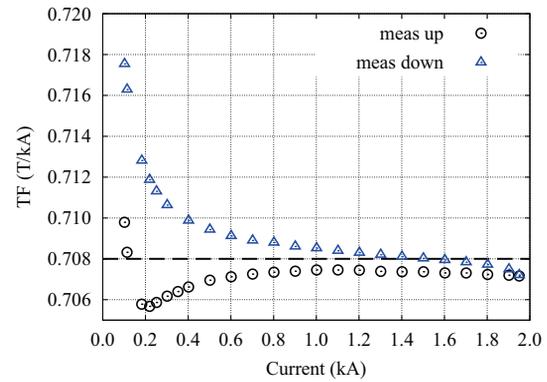

Figure 1: The measured dipole transfer function from the "DC loop" measurements. Circle: measured data during the up ramp after precycles. Triangle: measured data during the down ramp. The dashed line at 0.708 T/kA is the geometric value of the transfer function.

D96 spare dipole magnet. The effect is negligible for higher orders of non-allowed harmonics. Here we focus on the allowed harmonics where the persistent current effect is more significant.

MODEL VALIDATION

We compare the calculated allowed harmonics with the "DC loop" data measured between 50 and 1948 A. Figure 2 compares the dipole field transfer function. The up ramp was calculated with the $J_c(B)$ data from the up ramp branch of the measured strand magnetization. The down ramp was calculated with the $J_c(B)$ from the down ramp branch of the strand magnetization [12]. The calculation agrees reason-
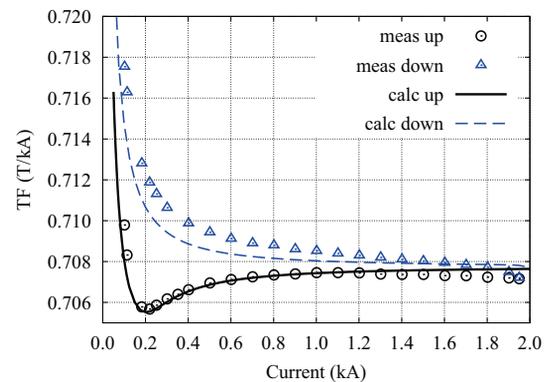

Figure 2: Comparison between the measured and calculated transfer function. Circle: measured data during the up ramp after precycles. Triangle: measured down ramp. Black line: calculated up ramp. Blue line: calculated down ramp.

ably well with the measurements, in particular the up ramp branch below 600 A. Similar agreement is also observed for b_3 (Fig. 3), b_5 (Fig. 4) and higher order allowed harmonics up to the 30-pole ($n = 15$). The good agreement validates the calculation model.
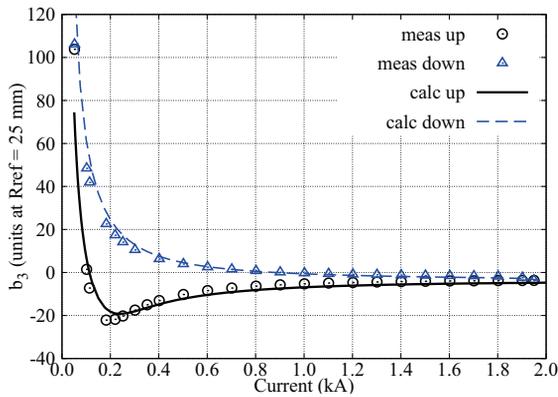
Figure 3: Comparison between the measured and calculated b_3. R_{ref} = 25 mm. Circle: measured data during the up ramp after precycles. Triangle: measured down ramp. Black line: calculated up ramp. Blue dashed line: calculated down ramp.
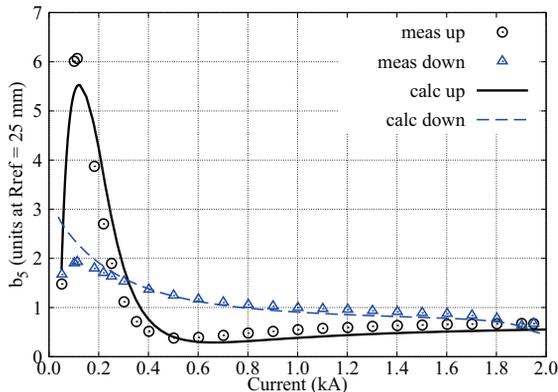

Figure 4: Comparison between the measured and calculated b_5. R_{ref} = 25 mm.
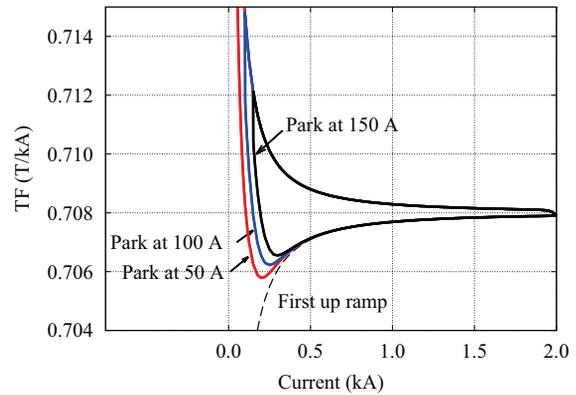

Figure 5: Impact of park currents on the dipole transfer function. Three park currents are calculated: 50, 100, and 150 A.
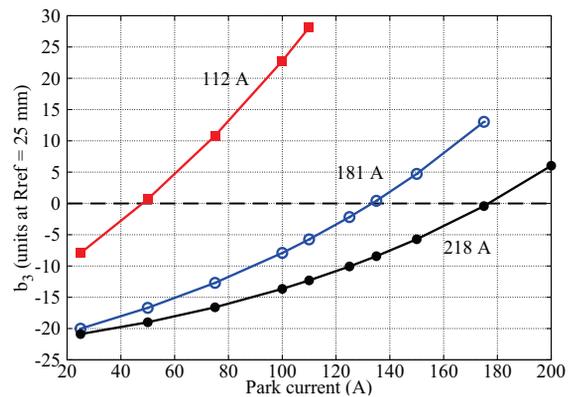

Figure 6: b_3 as a function of park current at three operation currents: 112, 181, and 218 A. An offset of -3.67 units for the geometric and saturation effect based on the measurements from the spare D96 magnet was applied to the calculation. R_{ref} = 25 mm.

EFFECT OF THE PARK CURRENTS

We can vary the persistent current effects on the harmonics by adjusting the park current from which the current starts ramping up toward the operation current after the down ramp. With the validated model, we calculate the persistent current effects on the allowed harmonics at different park currents. Figure 5 shows an example of the impact of park current on the dipole transfer function. As expected, the hysteresis of the transfer function at low current reduces with increasing park currents because the strand J_c decreases with the magnetic field.

For the impact on the high-order field errors, we consider three operation currents, 112, 181 and 218 A. Figure 6 shows the b_3 at each of the three operation levels as a function of park current. The intersections with the dashed line give the park current to reach zero b_3 at each operation current, e.g., 50 A park current for operation at 112 A.

CONCLUSIONS

Strong non-linear magnetic fields are observed for the RHIC arc dipoles operated at low currents (112 to 218 A).

The non-linear effects are due to the persistent currents in the NbTi superconducting filaments in the magnet conductors. Using the critical state model, we calculated the persistent current effects and achieved good agreement with the measured steady-state field errors (allowed terms) on a spare arc dipole magnet between 50 and 1948 A at 4.3 K. Based on the calibrated model, we calculated the persistent current effects on the allowed harmonics as a function of park current at three possible operation currents. We expect a zero b_3 at 112 A with a park current of 50 A. The developed model can be used for understanding the persistent current effects in the arc dipole magnets for the low energy RHIC operation.

REFERENCES

[1] M. Anerella *et al.*,"The RHIC magnet system," *Nuclear Instruments and Methods in Physics Research Section A: Accelerators, Spectrometers, Detectors and Associated Equipment*, vol. 499, no. 2-–3, pp. 280–315, 2003.

[2] K.-H. Mess, P. Schmüser, and S. Wolff, *Superconducting accelerator magnets*. World Scientific, 1996, ch. 6.

[3] S. Caspi, W. Gilbert, M. Helm, and L. J. Laslett, "The effects of filament magnetization in superconducting magnets as calculated by Poisson," *IEEE Transactions on Magnetics*, vol. 23, no. 2, pp. 510–513, March 1987.

[4] C. Völlinger, M. Aleksa, and S. Russenschuck, "Calculation of persistent currents in superconducting magnets," *Phys. Rev. ST Accel. Beams*, vol. 3, p. 122402, Dec 2000.

[5] S. Russenschuck, *Field Computation for Accelerator Magnets: Analytical and Numerical Methods for Electromagnetic Design and Optimization*. Weinheim: John Wiley & Sons, 2010.

[6] V. Kashikhin and A. Zlobin, "Calculation of coil magnetization effect in superconducting accelerator magnets," Fermi National Accelerator Laboratory, Tech. Rep. TD-00-010, February 2000.

[7] X. Wang *et al.*, "Validation of finite-element models of persistent-current effects in Nb$_3$Sn accelerator magnets," *IEEE Trans. Appl. Supercond.*, vol. 25, no. 3, p. 4003006, 2015.

[8] S. Izquierdo Bermudez, L. Bottura, and E. Todesco, "Persistent-current magnetization effects in high-field superconducting accelerator magnets," *IEEE Trans. Appl. Supercond.*, vol. 26, no. 4, p. 4003905, 2016.

[9] C. P. Bean, "Magnetization of hard superconductors," *Physical Review Letters*, vol. 8, pp. 250–253, Mar. 1962.

[10] Y. B. Kim, C. F. Hempstead, and A. R. Strnad, "Critical persistent currents in hard superconductors," *Physical Review Letters*, vol. 9, pp. 306–309, Oct. 1962.

[11] M. N. Wilson, *Superconducting Magnets*, Oxford University Press, 1983, ch. 8.2.3, p. 165.

[12] X. Wang *et al.*, "Persistent current effects in RHIC arc dipole magnets for low energy operation," Lawrence Berkeley National Laboratory Superconducting Magnet Program, Tech. Rep. 2016-0921, 2016.

[13] D. E. Knuth and T. J. Buckholtz, "Computation of tangent, Euler, and Bernoulli numbers," *Mathematics of Computation*, vol. 21, pp. 663–688, 1967.

[14] S. Le Naour, "Test report on magnetization measurements made on RHIC wires with CERN test station," CERN, Tech. Rep. 2003-03, 2003.

[15] N. Schwerg and C. Vollinger, "Development of a current fit function for NbTi to be used for calculation of persistent current induced field errors in the LHC main dipoles," *IEEE Trans. Appl. Supercond.*, vol. 16, no. 2, pp. 1828–1831, June 2006.

[16] A. K. Jain, "Harmonic coils," in *Proceedings of CERN accelerator school on measurement and alignment of accelerator and detector magnets*, April 1997.

[17] A. K. Jain, "Basic theory of magnets," in *Proceedings of CERN accelerator school on measurement and alignment of accelerator and detector magnets*, April 1997.